Host Genetic Background and Gut Microbiota Contribute to Differential Metabolic Responses to Fructose Consumption in Mice

In Sook Ahn[1,8], Jennifer M. Lang[2,8], Christine A. Olson[1], Graciel Diamante[1], Guanglin Zhang[1], Zhe Ying[1], Hyae Ran Byun[1], Ingrid Cely[1], Jessica Ding[1], Peter Cohn[1], Ira Kurtz[3,4], Fernando Gomez-Pinilla[1,5], Aldons J. Lusis[2], Elaine Y. Hsiao[1], and Xia Yang[1,4,6,7*]

[1] Department of Integrative Biology and Physiology, University of California, Los Angeles, CA

[2] Department of Medicine/Division of Cardiology, David Geffen School of Medicine, University of California, Los Angeles, CA

[3] Department of Medicine, Division of Nephrology, University of California, Los Angeles, CA

[4] Brain Research Institute, University of California, Los Angeles, CA

[5] Department of Neurosurgery, University of California, Los Angeles, CA

[6] Molecular Biology Institute, University of California, Los Angeles, CA

[7] Institute for Quantitative and Computational Biosciences, University of California, Los Angeles, CA

[8] These authors contributed equally

***Corresponding author:** Xia Yang, Ph.D.

Department of Integrative Biology and Physiology, University of California, Los Angeles

Los Angeles, CA 90095, USA

Tel: (310) 206-1812, Email: xyang123@ucla.edu

300 words (Abstract), 4923 words (Main text), 2 Tables, and 5 Figures

Running title: Gut Microbiota in Fructose Response

Footnotes:

Funding: XY and FG-P are funded by NIH DK104363. JML was supported by NIH T32 DK007789. GD was supported by NIEHS NIH T32ES015457 and American Diabetes Association Postdoctoral Fellowship 1-19-PDF-007-R. IK is supported in part by DK077162, the Allan Smidt Charitable Fund, and the Factor Family Foundation Chair in Nephrology. AL is supported by NIH HL28481 and HL30568. CAO is supported by NIA F31AG064844. EYH is supported by DoD ARO W911NF1710402 and is a New York Stem Cell Foundation – Robertson Investigator.

Author disclosures: The authors report no conflicts of interest.

Supplemental Figures 1-5 are available from the "Supplementary data" link in the online posting of the article and from the same link in the online table of contents at https://academic.oup.com/jn/. Supplemental Tables 1 and 2 were uploaded separately as excel files at https://figshare.com/s/ff6ffce17c10f6a1eb1f

To whom correspondence should be addressed. Email: xyang123@ucla.edu

Abbreviations used: AM, *Akkermansia muciniphila*; AUC, area under the curve; B6, C57BL/6J; DBA, DBA/2J; FDR, false discovery rate; FMT, fecal microbiota transplant; FVB, FVB/NJ; IPGTT, intraperitoneal glucose tolerance test; PCoA, principal coordinates analysis; PERMANOVA, permutational multivariate analysis of variance; TH, tyrosine hydrogenase

ABSTRACT

Background: It is unclear how high fructose consumption induces disparate metabolic responses in genetically diverse mouse strains.

Objective: We aim to investigate whether the gut microbiota contributes to differential metabolic responses to fructose.

Methods: Eight-week-old male C57BL/6J (B6), DBA/2J (DBA), and FVB/NJ (FVB) mice were given 8% fructose solution or regular water (control) for 12 weeks. The gut microbiota composition in cecum and feces was analyzed using 16S rDNA sequencing, and PERMANOVA was used to compare community across mouse strains, treatments, and time points. Microbiota abundance was correlated with metabolic phenotypes and host gene expression in hypothalamus, liver and adipose tissues using Biweight midcorrelation. To test the causal role of the gut microbiota in determining fructose response, we conducted fecal transplants from B6 to DBA mice and vice versa for 4 weeks, as well as gavaged antibiotic-treated DBA mice with *Akkermansia* for 9 weeks, accompanied with or without fructose treatment.

Results: Compared to B6 and FVB, DBA mice had significantly higher Firmicutes/Bacteroidetes ratio and lower baseline levels of *Akkermansia* and S24-7 ($P < 0.05$), accompanied by metabolic dysregulation after fructose consumption. Fructose altered specific microbial taxa in individual mouse strains, such as a 7.27-fold increase in *Akkermansia* in B6 and 0.374-fold change in Rikenellaceae in DBA (FDR < 5%), which demonstrated strain-specific correlations with host metabolic and transcriptomic phenotypes. Fecal transplant experiments indicated that B6 microbes conferred resistance to fructose-induced weight gain in DBA mice ($F = 43.1$, $P < 0.001$), and *Akkermansia* colonization abrogated the fructose-induced weight gain ($F = 17.8$, $P < 0.001$) and glycemic dysfunctions ($F = 11.8$, $P = 0.004$) in DBA mice.

Conclusions: Our findings support that differential microbiota composition between mouse strains is partially responsible for host metabolic sensitivity to fructose, and that *Akkermansia* is a key bacterium that confers resistance to fructose-induced metabolic dysregulation.

Keywords: gut microbiota, fructose, metabolic syndrome, fecal transplant, *Akkermansia,* microbiota-host interaction, gene by diet interaction

30 **Introduction**

31 The drastic increase in fructose consumption over the past few decades has been paralleled by
32 the rising prevalence of metabolic syndrome and diabetes (1). Our recent systems nutrigenomics
33 study unraveled the impact of fructose on transcriptome, epigenome and gene-gene interactions
34 in the hypothalamus, which is the main regulator of metabolism (2). Additionally, studies on the
35 liver and adipose tissues have also revealed fructose-induced alterations in genes involved in
36 several aspects of systemic metabolism (3–5). Interestingly, genetically diverse mouse strains
37 demonstrate disparate metabolic responses to fructose consumption, a finding reproducible
38 across multiple studies, including ours (5,6). However, the causal mechanisms underlying the
39 inter-individual differences in metabolic responses to fructose have yet to be elucidated.

40 The gut microbiome is emerging as an important modulator of metabolism, obesity, and
41 other metabolic disorders (7). Its dynamic nature, ease of manipulation, and response to dietary
42 intervention have made the gut microbiome a suitable therapeutic target to mitigate metabolic
43 syndrome (8). Diet influences trillions of gut microorganisms as early as one day post dietary
44 intervention (9). The gut microbiome has been suggested to contribute to phenotypic diversity in
45 different mouse strains on a high-fat high-sucrose diet (10,11). It is plausible that the gut
46 microbiome also plays a role in determining inter-individual variability in metabolic responses to
47 fructose consumption.

48 Dietary fructose is mainly absorbed in the small intestine, where it can be extensively
49 metabolized into glucose and organic acids. However, excessive amount of fructose that is not
50 absorbed in the small intestine due to malabsorption or high intake can undergo colonic bacterial
51 fermentation, resulting in the production of metabolites such as short-chain fatty acids (12).
52 Fructose also has the potential to modify the microbiota community and its normal function. For

53 instance, fructose metabolites can shape the gut environment and be an energy source for the gut
54 microbiota (13). Fructose can also suppress gut bacterial colonization by silencing a colonization
55 factor in a commensal bacterium (14).

56 Here, we investigated gut microbiota as a potential link between fructose consumption
57 and differential metabolic phenotypes in mice with diverse genetic backgrounds. We tested our
58 paradigm in three mouse strains, namely C57BL/6J (B6), DBA/2J (DBA), and FVB/NJ (FVB),
59 which have contrasting metabolic susceptibility to high caloric diets (5,6,11).

60

61 **Methods**

62 **Animals and study design**

63 To investigate the role of the gut microbiota in host responses to fructose consumption, we
64 examined microbial composition in the context of differential metabolic and transcriptomic
65 responses in multiple mouse strains (**Supplemental Figure 1**). Seven-week-old male mice (20-
66 25g) from three inbred strains, namely B6, DBA, and FVB, were obtained from the Jackson
67 Laboratory (Bar Harbor, ME) and housed in a pathogen-free barrier facility with a 12-hour
68 light/dark cycle at University of California, Los Angeles. Mice were fed Lab Rodent Diet 5001,
69 containing 234 g/kg protein, 45 g/kg fat, 499 g/kg carbohydrate, and 2.89 kcal/g metabolizable
70 energy (LabDiet, St. Louis, MO). After a one-week acclimation period, mice from each strain
71 were randomly divided into two groups. One group was provided with regular water (control
72 group, *n*=8-10 mice/strain) and the other group was given 8% (w/v) fructose (3.75 kcal/g energy;
73 NOW Real Food, Bloomingdale, IL) dissolved in regular water (fructose group, *n*=10-12
74 mice/strain) for 12 weeks *ad libitum*. Food and drink intake were monitored daily on a per-cage
75 basis. Distinct alterations in body weight, fat mass, plasma lipids, glycemic traits, intraperitoneal

76 glucose tolerance test (IPGTT), and the transcriptome of liver, adipose, and hypothalamus in
77 response to fructose consumption across mouse strains were observed and previously published
78 (5). Gut microbiota composition of cecal and fecal samples were analyzed. Fructose-responsive
79 microbiota were correlated with metabolic phenotypes and host gene expression to prioritize
80 microbial taxa that may contribute to differential host fructose responses. Lastly, fecal
81 microbiota transplant (FMT) and *Akkermansia muciniphila* (AM) colonization experiments were
82 conducted to test the causal role of gut microbiota in determining mouse strain-specific fructose
83 responses. The study was performed in accordance with National Institutes of Health Guide for
84 the Care and Use of Laboratory Animals. All experimental protocols were approved by the
85 Institutional Animal Care and Use Committee at the University of California, Los Angeles.
86

87 **Fecal and cecal microbiota analysis**

88 Feces were collected at 1, 2, 4, and 12 weeks of fructose treatment, and cecal contents were
89 collected at the end of fructose treatment (12 weeks). Samples were snap frozen and then stored
90 at -80°C until DNA isolation. Microbial DNA was isolated from samples using the MO BIO
91 PowerSoil®-htp 96 Well Soil DNA Isolation Kit (MO BIO, Carlsbad, CA). For the fecal and
92 cecal samples, the same lot isolation kit was used; for the fecal transplant samples a different lot
93 kit was used. The V4 region (15,16) of the 16S rDNA gene was amplified in triplicate with
94 barcoded primers (515f and 806r) (17). PCR products were quantified with Quant-iTTM
95 PicoGreen® dsDNA Assay Kit (Thermo Fisher Scientific) and all samples from a specific
96 experiment (e.g., fecal, cecal, or fecal transplant experiment) were combined in equal amounts
97 (~250 ng per sample) into a single pooled submission to be purified with the UltraClean PCR®
98 Clean-Up Kit (MO BIO). Single-end reads were generated on the Illumina HiSeq 2500 platform

99 using two lanes for each pool of mixed samples to create an unbiased sequencing approach.
100 Roughly 500 samples were sequenced per submission, and each dataset of fecal, cecal, and fecal
101 transplant samples were sequenced in different submissions. Raw sequences were processed
102 using QIIME to produce de-multiplexed and quality-controlled sequences. Reads were binned
103 into OTUs at 97% similarity using UCLUST against the Greengenes reference database (18).
104 Singletons, OTUs representing less than 0.005% total relative abundance, unsuccessfully
105 sequenced samples, and outliers were removed. Samples were normalized to a rarefied level
106 specific for each dataset to reduce the effect of unequal sequencing depth to result in 60,000,
107 106,815, and 37,614 reads per sample for fecal, cecal, and fecal transplant samples, respectively.
108 A total of 180 fecal, 46 cecal, and 170 fecal transplant samples were used for downstream
109 analysis.
110

111 **Correlation analysis between gut microbiota and metabolic phenotypes or fructose**
112 **signature genes**

113 Correlation analysis was performed between the relative abundance or proportion of microbiota
114 with metabolic phenotypes including body weight, adiposity, and area under the curve (AUC) for
115 glucose tolerance. Microbiota proportions were also correlated with differentially expressed
116 genes in response to fructose consumption, or "fructose signature genes", in hypothalamus, liver,
117 and adipose tissue. The fructose signature genes correlated with bacterial abundance were
118 classified for their biological functions in Gene Ontology, REACTOME, and KEGG using the
119 GSEA tool (19).
120

121 **Antibiotics treatment prior to fecal transplant or *Akkermansia* colonization**

122 Six-week-old B6 or DBA recipient mice were orally gavaged with a solution of vancomycin (50
123 mg/kg), neomycin (100 mg/kg), and metronidazole (100 mg/kg) twice daily for 7 days.
124 Ampicillin (1 mg/mL) was also provided *ad libitum* in drinking water (20). Antibiotic-treated
125 mice were housed in sterile cages with sterile water and food throughout the experiment.
126 Following antibiotics treatment, mice were used in either fecal transplant or *Akkermansia*
127 colonization experiments, as described below.
128

129 **Fecal transplant between B6 and DBA mice**

130 Reciprocal fecal transplant between B6 and DBA mice was conducted. B6 mice receiving DBA
131 feces were designated as B6(DBA) and DBA mice receiving B6 feces were designated as
132 DBA(B6). To serve as control groups, DBA mice were transplanted with DBA feces and
133 designated as DBA(DBA), and B6 mice were transplanted with B6 feces and designated as
134 B6(B6). Fecal transplant was performed according to previous studies with some modification
135 (21,22). Briefly, freshly collected feces were pooled from 4 donor mice and suspended at
136 40mg/mL concentration in anaerobic PBS. The suspension (150 μL) was orally gavaged to the
137 recipient mice for 4 weeks. Total time between collecting feces and delivery of microbial
138 contents into recipients was kept as short as possible (< 15 min) to protect anaerobes. After 1
139 week of fecal transplant, mice from each of the four transplant experiments, namely B6(DBA),
140 B6(B6), DBA(B6), DBA(DBA), were divided into two groups and treated with 8% fructose or
141 regular water for 12 weeks (n = 7-14 mice/group). Body weight and IPGTT were measured using
142 the methods described previously (5).
143

144 ***Akkermansia* colonization in DBA mice**

145 *Akkermansia* colonization was conducted according to Olson et al. (20). Antibiotic-treated DBA
146 mice were orally gavaged with 200 μL bacterial suspension (5 x 10^9 cfu/mL in anaerobic PBS)
147 throughout the experiment. After 1 week of bacterial gavage, DBA mice were treated with 8%
148 fructose or regular water for 8 weeks (n = 10-14/group). DBA mice receiving anaerobic PBS
149 served as control (n = 8-10/group). Body weight and IPGTT were measured as described
150 previously (5).
151
152 **Statistical analysis**
153 The microbiota data was summarized into relative abundance by taxonomic level in QIIME, and
154 communities were visualized with principal coordinates analysis (PCoA) based on the weighted
155 UniFrac distance measure (23). Categorical groups (treatment, time, mouse strain) were
156 confirmed to have similar multivariate homogeneity of group dispersions to allow them to be
157 compared using the non-parametric PERMANOVA (permutational multivariate analysis of
158 variance) test with the adonis function (24). Microbial composition was analyzed at the phylum,
159 family, and genus taxonomic levels using the Statistical Analysis of Metagenomic Profiles
160 (STAMP) software (25).
161 Linear discriminant analysis (LDA) effect size (LEfSe) was used to identify taxa
162 differentially represented between three mouse strains using standard parameters ($P < 0.05$, LDA
163 score > 2.0) (26). Using the identified features from the LEfSe analysis, we selected six fecal
164 genera which showed contrasting patterns in their baseline levels between DBA and the other
165 two mouse strains, B6 and FVB. To visualize the baseline differences of these six genera
166 between the three mouse strains, boxplots were plotted using centered log-ratio (CLR)
167 transformed values from OTU counts with the 'rgr' package in R software (24). The difference

168 between strains was assessed using a one-way ANOVA followed by Sidak's post hoc test.
169 Because *Turicibacter* was not normally distributed, the difference between strains was analyzed
170 by Kruskal-Wallis test followed by Dunn's test.

171 Taxa that differed between the fructose and regular water groups were identified using
172 White's non-parametric T-test (27), followed by Storey's false discovery rate (FDR) estimation
173 using relative abundance data and the Statistical Analysis of Metagenomic Profiles (28). A one-
174 way ANOVA followed by Sidak's post hoc test was used to determine the difference in
175 Firmicutes/Bacteroidetes (F/B) ratio between three mouse strains. F/B ratio was calculated by
176 dividing the proportion of Firmicutes and Bacteroidetes for each sample, and then log-
177 transformed to achieve normal distribution.

178 Correlation between gut microbiota and metabolic phenotypes or fructose signature genes
179 from individual tissues, was assessed using Biweight midcorrelation (bicor) (29). Statistical *P*-
180 values were adjusted using the Benjamini-Hochberg approach and FDR < 0.05 was considered
181 significant.

182 To analyze body weight gain and glucose tolerance data involving multiple time points in
183 fecal transplant and *Akkermansia* colonization experiments, a three-way repeated-measures
184 ANOVA followed by Sidak's post hoc test was used. The effects and interaction of three factors
185 (microbial manipulation, fructose, time) on the metabolic phenotypes were tested.

186 To evaluate the effects of fructose under each unique microbiota manipulation (e.g.,
187 within *Akkermansia*-colonized groups or within B6 mice transplanted with DBA microbe) across
188 multiple time points, a two-way repeated-measures ANOVA was used. Fructose treatment was
189 used as the between-group factor and time was used as the within-subject factor. To assess the
190 effect of a given microbiota manipulation under fructose treatment across multiple time points, a

191 two-way repeated-measures ANOVA was used. Microbiota manipulation was used as the
192 between-group factor and time was used as the within-subject factor. If the interaction was
193 significant, microbiota manipulations within each time point were compared by Sidak's post hoc
194 test. Statistical analyses were performed using STATISTICA (version 7, Statsoft Inc., Tulsa,
195 OK) and GraphPad Prism (version 8, GraphPad Software Inc., San Diego, CA). Data were
196 expressed as means ± SEM. $P < 0.05$ was considered statistically significant.
197

198 **Results**

199 **Strain-specific metabolic responses to fructose treatment**

200 We have previously reported that B6, DBA, and FVB mice demonstrated striking differences in
201 their metabolic responses to 8% fructose treatment for 12 weeks (5). DBA mice were more
202 sensitive to fructose in terms of obesity and diabetes-related phenotypes including body weight,
203 adiposity, and glucose intolerance. B6 mice showed significant increases while FVB mice had
204 decreases in plasma cholesterol levels. These results demonstrate strong inter-strain variability in
205 fructose response in genetically divergent mouse strains. Importantly, the disparate metabolic
206 responses were not due to differences in overall energy intake [14.6 ± 0.384, 17.9 ± 0.880, or
207 18.0 ± 0.403 kcal/(mouse · d) for B6, DBA, or FVB, respectively] (5). The differences in
208 metabolic responses (DBA > B6 or FVB) were also not correlated with the amount of fructose
209 water intake [FVB (23.6 ± 1.36 mL/(mouse · d) > B6 (8.74 ± 0.187 mL/(mouse · d) or DBA
210 (8.47 ± 0.390 mL/(mouse · d)] (5). Amount of intake was likely driven by differences in fructose
211 perception and preference between the mouse strains (6,30).
212

213 **Overall effects of fructose on gut microbiota community**

214 The gut microbiota in the three mouse strains was assessed using 16S rDNA sequencing. PCoA
215 plots showed distinct clusters of mouse strain for both the cecal ($P < 0.001$ by PERMANOVA,
216 **Figure 1**A) and the fecal samples ($P < 0.001$, Figure 1B). Time was also a significant factor in
217 fecal samples ($P < 0.001$), with week 12 separating from the earlier weeks when evaluating all
218 mouse strains together (Figure 1C) or each mouse strain separately (Figure 1D-F).
219 Fecal microbiota differences were seen between fructose and water groups at 12-weeks in
220 B6 ($P < 0.001$ by PERMANOVA, Figure 1G) and DBA mice ($P = 0.046$, Figure 1H), but not in
221 FVB ($P = 0.58$, Figure 1I). In cecum, the fructose group showed separation from controls for B6
222 mice (Figure 1J), however, the separation was not statistically significant with PERMANOVA
223 ($P = 0.43$). This result may be influenced by the difference in multivariate spread ($P = 0.038$)
224 since PERMANOVA assumes equal dispersion. Fructose treatment was a significant factor for
225 cecal microbiota composition in DBA ($P = 0.002$, Figure 1K), but not for FVB ($P = 0.44$, Figure
226 1L). Overall, consistent with the differential effects of fructose on metabolic phenotypes, DBA
227 gut microbiota in both feces and cecum were sensitive to fructose treatment.
228

229 **Baseline differences in gut microbiota between mouse strains show correlation with host**
230 **metabolic phenotypes**

231 Differences in baseline microbial composition can drive distinct host responses to the same
232 dietary manipulation (31,32). At the phylum level, there were no significant differences in cecum
233 Firmicutes/Bacteroidetes (F/B) ratios between the three mouse strains (**Figure 2**A**)**. However, in
234 fecal samples, DBA had significantly higher F/B ratio (1.78 ± 0.169) than B6 (0.346 ± 0.024, P
235 < 0.001 by one-way ANOVA) or FVB (0.898 ± 0.091, $P < 0.001$) (Figure 2B), agreeing with the
236 known association of higher Firmicutes abundance with obesity (33) and the increased adiposity

237 in DBA (5). The microbial taxa that accounted for the greatest differences between the three
238 mouse strains included 21 cecal (**Supplemental Figure 2**A, B) and 14 fecal (Supplemental
239 Figure 2C, D) microbial genera based on the LEfSe analysis.

240 We reasoned that if any specific microbial taxon determines the differential fructose
241 response between the mouse strains, its abundance likely shows contrasting patterns between the
242 susceptible strain DBA and the two resistant strains. Out of 21 cecal genera (Supplemental
243 Figure 2B**),** none showed contrasting patterns between DBA and the two resistant strains. Out of
244 the 14 fecal genera (Supplemental Figure 2D**)**, 6 showed distinct patterns in DBA mice
245 compared to the resistant strains (Figure 2C-H). DBA mice showed higher centered log-ratio
246 (CLR) abundance for *Lactobacillus*, an unknown bacteria of order Clostridiales, and an unknown
247 bacteria of family Lachnospiraceae compared to B6 and FVB. On the other hand, DBA mice had
248 lower CLR abundance for an unknown bacteria of family S24-7, *Akkerman*sia, and *Turicibacter*.
249 To understand the potential role of these microbial taxa in metabolic regulation, the correlations
250 between the proportion of these taxa and adiposity gain across all mouse strains were tested. We
251 found that all taxa were significantly correlated with adiposity gain ($P < 0.01$, Figure 2I-N).
252

253 **Fructose-responsive microbiota and correlation with host metabolic phenotypes**

254 Next, we explored the differentially abundant microbiota between fructose and water groups in
255 the three mouse strains at 12 weeks. We observed more fructose responsive microbiota in feces
256 (9 taxa) compared to cecum samples (1 taxon) across mouse strains at the family level (**Table 1**).

257 In feces, fructose treatment showed the highest impact in B6 mice by altering the
258 abundance of many microbiota (nine families and three genera). Significant decreases were
259 observed in five taxa belonging to phylum Firmicutes. There were also significant increases in

260 S24-7 of phylum Bacteroidetes and Verrucomicrobiaceae. Within the Verrucomicrobiaceae
261 family, *Akkermansia* significantly increased in B6 mice after fructose treatment. In DBA feces,
262 fructose altered the abundance of Rikenellaceae and Pseudomonadaceae. These two families
263 were also found to be fructose responsive in B6 mice, however, the response was more dramatic
264 in DBA mice (0.374-fold and 33.3-fold changes in DBA compared with 0.620-fold and 3.33-fold
265 changes in B6 for Rikenellaceae and Pseudomonadaceae, respectively). No fecal microbial taxa
266 were significantly altered by fructose in FVB mice (Table 1; **Supplemental Figure 3**A, B). In
267 DBA cecum, family Erysipelotrichaceae and two of its genera (*Clostridum* and an unknown
268 genus), and *Anaerostipes* were all significantly decreased by fructose. Fructose also significantly
269 increased cecal *Bifidobacterium* in FVB mice, while no cecal taxa were significantly changed in
270 B6 mice (Table 1; Supplemental Figure 3C, D).

271 We next correlated the abundance of these fructose-responsive taxa with metabolic
272 phenotypes in water or fructose-treated mice. In DBA mice, cecal Erysipelotrichaceae was
273 negatively correlated with adiposity and AUC (**Supplemental Figure 4**A, B). Fecal
274 Rikenellaceae in DBA mice had negative correlations with body weight and adiposity, and a
275 positive correlation with AUC in the fructose group, while no significant correlation was
276 observed with these phenotypes in the water group (**Figure 3**A-F). No phenotypic correlation
277 was observed for the fructose-responsive taxa in B6 and FVB mice, which is not surprising given
278 the weaker phenotypic alterations in these mouse strains in response to fructose consumption.
279

280 **Correlation of fructose-responsive microbiota with fructose signature genes in host**
281 **metabolic tissues**

282 We then analyzed the correlation between the abundance of fructose-responsive microbiota and
283 the host fructose signature genes in liver, adipose tissue, and hypothalamus (5). We observed
284 distinct correlation patterns in the three mouse strains: the B6 fructose-responsive taxa were
285 correlated with only hypothalamic fructose signature genes, while the fructose-responsive taxa in
286 DBA cecum or feces were correlated with only liver or adipose tissue signature genes,
287 respectively (summary in **Table 2**; full list of genes correlated with fructose-responsive taxa in
288 **Supplemental Table 1**).

289 In B6, *Dehalobacterium* showed positive correlation with hypothalamic genes encoding
290 the neurotransmitter transporter *Slc6a3*, a notch signaling component *Nrarp*, and an autophagy
291 gene *Atg3*. *Akkermansia* was correlated with several neurotransmitter related genes, including
292 *Oxt* encoding precursor of oxytocine/neurophysin 1 and *Th* encoding tyrosine hydroxylase. In
293 DBA cecum, both *Anaerostipes* and *Clostridium* were positively correlated with *Cyp8b1* in liver,
294 which is responsible for bile acid synthesis (34).

295 In DBA feces, all fructose-responsive taxa were correlated with host signature genes of
296 the adipose tissue, and these genes were involved in lipid metabolism, immune system, response
297 to lipid, cytokines, and hormone (**Supplemental Table 2)**. Adipose genes such as *Abhd3, Msr1,*
298 *Ccr1, Creb1,* and *Fas* were correlated with Rikenellaceae and Pseudomonadaceae as well as
299 genera within these families (Table 2; Supplemental Table 2). Taken together, these correlations
300 suggest that gut microbiota may interact with host genes in a mouse strain- and tissue-specific
301 manner in response to fructose.

302

303 **Alteration of gut microbiota modulates fructose response**

304 Since B6 and DBA mice showed disparate metabolic responses to fructose, we tested whether
305 B6 microbiota confers resistance and DBA microbiota confers vulnerability to fructose effects by
306 transplanting B6 feces to antibiotic-treated DBA mice and vice versa (**Figure 4**A). Using 16S
307 rDNA sequencing, we confirmed that the recipient mice gut microbiome shifted after fecal
308 transplant (**Supplemental Figure 5**A, B).

309 When the main effects of FMT, fructose, and time were tested, there were significant
310 FMT effects on weight gain in both B6 ($P < 0.001$, Figure 4B) and DBA mice ($P = 0.002$ Figure
311 4C), but there was no effect of FMT on glucose tolerance in both mouse strains (Figure 4D, E).
312 Overall, there was a significant fructose effect on weight gain in DBA mice ($P = 0.025$; Figure
313 4C), which was not observed in B6 mice (Figure 4B). In those fed fructose, body weight gain in
314 DBA mice receiving B6 bacteria [DBA(B6)] was significantly lower compared to DBA(DBA) at
315 4 weeks ($P = 0.028$), 6 weeks ($P = 0.006$), and 8 weeks ($P = 0.007$). In contrast, there was no
316 significant fructose effect in B6 mice receiving DBA bacteria [B6(DBA)] or in B6(B6) mice
317 (Figure 4B). These results suggest that DBA microbiota failed to induce fructose sensitivity in
318 B6 mice. On the other hand, DBA(B6) mice no longer displayed fructose-induced weight gain
319 (fructose effect $P = 0.66$) as seen in DBA(DBA) mice (fructose effect $P = 0.047$, Figure 4C),
320 supporting that B6 microbiota conferred resistance to body weight gain upon fructose
321 consumption.

322 The result from FMT experiment supports a causal role of B6 microbiota in conferring
323 fructose resistance to DBA. We next focused on prioritizing the potential microbes in B6 that
324 may determine the fructose resistance phenotype. *Akkermansia* was found to be a highly
325 plausible candidate to explain the dampened response to fructose in B6 for the following reasons.
326 First, *Akkermansia* has been previously demonstrated to carry anti-obesity and insulin sensitizing

327 effects (32,35,36). The beneficial effect of *Akkermansia* was also previously observed in mice
328 fed a high-fat/high-sucrose diet (37). Secondly, it was depleted in the vulnerable strain DBA but
329 was highly abundant in both resistant mouse strains, B6 and FVB (Figure 2G). Thirdly, fructose
330 treatment caused an increase in *Akkermansia* in B6 mice (Table 1; Supplemental Figure 3A).
331 Lastly, *Akkermansia* abundance in B6 is significantly correlated with a large number of
332 hypothalamic genes such as *Oxt* and *Th* that regulate metabolism (Table 2; Supplemental Table
333 1).

334 To test the role of *Akkermansia* in protecting against fructose-induced metabolic
335 dysregulation as predicted above, we gavaged DBA mice with *Akkermansia muciniphila* (AM)
336 or PBS media along with fructose treatment for 8 weeks (**Figure 5**A). There were significant
337 effects of AM on both body weight gain ($P < 0.001$) and glucose tolerance ($P < 0.001$) (Figure
338 5B, C). Under fructose treatment, DBA mice receiving AM had significantly lower weight gains
339 at 3 ($P = 0.023$) and 5-8 weeks ($P < 0.01$) compared to control mice receiving PBS. No AM
340 effect was observed in the water treatment mice ($P = 0.14$). Within AM or PBS group, fructose
341 had significant effects on body weight gain in the PBS control group ($P = 0.037$), whereas DBA
342 mice receiving AM no longer displayed fructose-induced body weight gain as seen in control
343 mice (Figure 5B). Furthermore, fructose increased glucose intolerance in PBS control group
344 (fructose effect $P = 0.044$), whereas AM treatment abrogated fructose-induced glucose
345 intolerance in DBA mice (Figure 5C). These results support that *Akkermansia* confers resistance
346 to fructose-mediated metabolic dysregulation.

347

348 **Discussion**

349 Our previous study showed that three mouse strains representing a range of genetic diversity
350 differed in their metabolic and transcriptomic responses to high fructose treatment (5). Since gut
351 microbiota is an important modulator of metabolic capacity (7), here we tested the hypothesis
352 that disparate fructose responses among mouse strains were at least partially driven by the gut
353 microbiota. Our 16S rDNA sequencing analysis revealed that baseline microbiota composition
354 and its response to fructose varied by mouse strains. The fecal transplant data indicates that B6
355 mice carry microbiota that confer resistance to fructose-induced body weight gain. We next
356 evaluated candidate taxa to explain the dampened response to fructose in B6 mice. We
357 prioritized *Akkermansia* since it is enriched in B6 compared to DBA mice, which have lower
358 levels. Indeed, gavaging *Akkermansia muciniphila* to DBA mice mitigated fructose-induced
359 obesity and glucose intolerance. These results support a causal role of gut microbiota in
360 determining the differential metabolic responses to fructose among genetically diverse mouse
361 strains.

362 As initial colonizing microbial species are important for establishing a favorable
363 environment for bacterial growth in a particular context (38), differences in baseline microbial
364 composition between mouse strains can lead to variations in the metabolic processes of
365 individuals in response to diet (31,32). We found that *Akkermansia*, *Turicibacter*, and S24-7
366 were lower in DBA mice but were abundant in B6 and FVB mice. On the other hand, the
367 baseline levels of *Lactobacillus,* Clostridiales and Lachnospiraceae were higher in DBA mice.
368 Previously, *Akkermansia* has been associated with obesity resistance and improved metabolic
369 parameters in humans and mice, and beneficial effects of dietary interventions have been
370 associated with the higher abundance of *Akkermansia* at baseline (32,36). S24–7 has protective
371 association against diabetes, whereas Lachnospiraceae promotes pathogenesis of diabetes in

372 NOD mice (39). The observed lack of protective *Akkermansia* and S-24, along with the higher
373 abundance in pathogenic Lachnospiraceae in DBA mice, agrees with the vulnerability of DBA
374 mice to fructose-induced metabolic dysregulation. Therefore, these bacterial taxa that differ
375 significantly at baseline between strains have the potential to regulate the differential response to
376 fructose treatment.

377 In addition to differences in baseline microbes that can explain inter-mouse strain
378 variability, bacteria altered by fructose may also play a role in the variability in metabolic
379 responses to fructose. It has been suggested that fructose shifts the gut microbiota and leads to a
380 westernized microbiome acquisition with altered metabolic capacity, resulting in development of
381 obesity or metabolic disorders (40). In our study, we found various microbes with significantly
382 altered abundances in DBA and B6 but not FVB, which may relate to their differential sensitivity
383 to fructose. Cecal Erypsipelotricaceae and *Anaerostipes* in DBA mice decreased in abundance
384 upon fructose consumption (Table 1; Supplemental Figure 3), and they are known as butyrate-
385 producing bacteria (41). Butyrate promotes the intestinal barrier development, and decreased
386 butyrate production can increase intestinal permeability (42). In both the B6 and DBA feces, we
387 also detected decreased abundance of Rikenellaceae and increased abundance of
388 Pseudomonadaceae following fructose treatment (Table 1). Increases in Pseudomonadaceae and
389 *Pseudomonas* were previously found in obese individuals with higher insulin resistance (43).
390 Therefore, despite the numerous differences between B6 and DBA, there were shared microbial
391 changes in response to fructose consumption. The weaker phenotypic responses in B6 can be a
392 result of compensatory balancing effects of higher abundances of beneficial bacteria such as
393 *Akkermansia* and S24-7 in B6.

394 We detected more fructose-responsive microbiota in B6 mice than in DBA and FVB
395 mice (Table 1), and, interestingly, most of these B6 taxa were associated with the hypothalamic
396 fructose signature genes (Table 2; Supplemental Table 1). Among them are genes that are
397 important for energy homeostasis such as *Nrarp, Qxt*, and *Th*. *Nrarp* encodes an intracellular
398 component of the Notch signaling pathway and regulates differentiation of mouse hypothalamic
399 arcuate neurons responsible for feeding and energy balance. Dysregulation of this homeostatic
400 mediator is an underlying cause of various diseases ranging from growth failure to obesity (44).
401 *Qxt* encodes oxytocin which is the anorexigenic peptide. Oxytocin maintains homeostasis in
402 feeding-related behavior (45). *Th* gene encodes tyrosine hydrogenase (TH). Hypothalamic
403 arcuate nucleus TH neurons play a role in energy homeostasis, and silencing of TH neurons
404 reduces body weight (46). Our previous mice study (2) reported that fructose is an inducer of
405 both genomic and epigenomic variability in hypothalamus and has the ability to reorganize gene
406 networks that plays a central role in metabolic regulation and neuronal processes. The current
407 study suggests that fructose-induced transcriptomic changes in the hypothalamus of B6 mice
408 could be partly driven by fructose-responsive gut microbiota.

409 In contrast to B6 mice, fructose-responsive microbiota in DBA mice were associated with
410 lipid and inflammatory genes in the adipose tissue (Table 2; Supplemental Table 2). *Abhd3* is a
411 crucial factor for insulin resistance in adipose tissue (47); *Sema3e* contributes to inflammation
412 and insulin resistance in obese mice (48); *Msr1* is macrophage scavenger receptor 1 and provides
413 protection from excessive insulin resistance in obese mice (49); *Creb1* promotes expression of
414 transcriptional factors of adipogenesis and insulin resistance in obesity (50); *Fas* contributes to
415 adipose tissue inflammation, hepatic steatosis, and insulin resistance induced by obesity (51).
416 Therefore, these adipose-tissue genes correlating with fructose-responsive bacteria in DBA are

417 relevant to the increased adiposity and compromised insulin sensitivity seen in DBA mice.
418 However, we acknowledge that the correlative relationship observed here does not directly imply
419 causation, and future experiments are needed to directly test the causal role of the genes as well
420 as the bacteria implicated.

421 Our fecal transplant study support that B6 mice carry gut microbes that confer resistance
422 to fructose-induced metabolic syndrome, while DBA microbiota did not significantly induce
423 fructose sensitivity in B6 mice. We further demonstrate that *Akkermansia* partially mediates the
424 protective effect of B6 microbiota. This is the first time that *Akkermansia* is implicated in
425 determining fructose response. Given the recognized therapeutic potential of modulating the gut
426 microbiota (8), probiotic treatment with *Akkermansia* may represent a viable approach to
427 mitigate fructose-induced metabolic abnormalities. In addition to *Akkermansia,* other bacteria
428 may also play roles in modulating the differential fructose response between individuals. Future
429 efforts will explore the pathogenic or protective roles of other bacterial species, such as
430 *Lactobacillus*, *Turicibacter*, or *Pseudomonas*.

431 In summary, our multi-strain, multi-omics (gut microbiome, transcriptome, and
432 phenome) integrative studies of inter-individual variability in fructose-induced metabolic
433 syndrome established a causal role of gut microbiota in modulating host responses to fructose, a
434 significant metabolic risk in modern societies. Importantly, our study identified key microbial
435 species that may serve as preventative or therapeutic targets for metabolic syndrome. By
436 exploring gut-host interactions, our study also opens numerous hypotheses regarding specific
437 microbiota-host interactions to be further elucidated in the future.
438

Acknowledgements

The authors thank Dr. Richard C. Davis for assistance of oral gavage and fecal transplant, Dr. Yuqi Zhao and Dr. Zeyneb Kurt for the assistance with data analysis, and Dr. Sana Majid, Paul Patel, Maya Singh, Jessica Yang and Justin Yoon for helping with animal experiments.

XY, EYH, ISA, and CO designed the research; ISA, CAO, JML, ZY, IC, GD, PC, HRB and JD conducted research including animal experiments; JML, ISA, GZ, IK, JD analyzed data; ISA, XY and JML wrote the manuscript; FG-P, AL and all authors contributed to manuscript revision; XY had primary responsibility for the final content; All authors read and approved the final version of the paper.

References

1. Basciano H, Federico L, Adeli K. Fructose, insulin resistance, and metabolic dyslipidemia. Nutr Metab. 2005;2:1–14.
2. Meng Q, Ying Z, Noble E, Zhao Y, Agrawal R, Mikhail A, Zhuang Y, Tyagi E, Zhang Q, Lee JH, et al. Systems nutrigenomics reveals brain gene networks linking metabolic and brain disorders. EBioMedicine. 2016;7:157–66.
3. Koo HY, Wallig MA, Chung BH, Nara TY, Cho BHS, Nakamura MT. Dietary fructose induces a wide range of genes with distinct shift in carbohydrate and lipid metabolism in fed and fasted rat liver. Biochim Biophys Acta - Mol Basis Dis. 2008;1782:341–8.
4. Li Z, Xiong C, Mo S, Tian H, Yu M, Mao T, Chen Q, Luo H, Li Q, Lu J, et al. Comprehensive transcriptome analyses of the fructose-fed syrian golden hamster liver provides novel insights into lipid metabolism. PLoS One. 2016;11:1–19.
5. Zhang G, Byun HR, Ying Z, Blencowe M, Zhao Y, Hong J, Shu L, Chella Krishnan K, Gomez-Pinilla F, Yang X. Differential metabolic and multi-tissue transcriptomic responses to fructose consumption among genetically diverse mice. Biochim Biophys Acta - Mol Basis Dis. Elsevier; 2020;1866:165569.
6. J. Glendinnning, L. Breinager, E. Kyrillou, K. Lacuna, R. Rocha AS. Differential effects of sucrose and fructose on dietary obesity in four mouse strains. Physiol Behav. 2010;101:331–43.
7. Turnbaugh PJ, Ley RE, Mahowald M a, Magrini V, Mardis ER, Gordon JI. An obesity-associated gut microbiome with increased capacity for energy harvest. Nature. 2006;444:1027–31.
8. Fändriks L. Roles of the gut in the metabolic syndrome: an overview. J Intern Med. 2016;1–18.
9. David LA, Maurice CF, Carmody RN, Gootenberg DB, Button JE, Wolfe BE, Ling A V, Devlin AS, Varma Y, Fischbach MA, et al. Diet rapidly and reproducibly alters the human gut microbiome. Nature. 2014;505:559–63.
10. Carmody RN, Gerber GK, Luevano JM, Gatti DM, Somes L, Svenson KL, Turnbaugh PJ. Diet dominates host genotype in shaping the murine gut microbiota. Cell Host Microbe. Elsevier Inc.; 2015;17:72–84.
11. Parks BW, Nam E, Org E, Kostem E, Norheim F, Hui ST, Pan C, Civelek M, Rau CD, Bennett BJ, et al. Genetic control of obesity and gut microbiota composition in response to high-fat, high-sucrose diet in mice. Cell Metab. 2013;17:141–52.
12. Oh JH, Alexander LM, Pan M, Schueler KL, Keller MP, Attie AD, Walter J, van Pijkeren JP. Dietary fructose and microbiota-derived short-chain fatty acids promote bacteriophage production in the gut symbiont Lactobacillus reuteri. Cell Host Microbe. 2019;25:273–84.
13. Ríos-Covián D, Ruas-Madiedo P, Margolles A, Gueimonde M, De los Reyes-Gavilán CG, Salazar N. Intestinal short chain fatty acids and their link with diet and human health. Front Microbiol. 2016;7:1–9.
14. Townsend GE, Han W, Schwalm ND, Raghavan V, Barry NA. Dietary sugar silences a colonization factor in a mammalian gut symbiont. 2019;116:233–8.
15. Faith JJ, Guruge JL, Charbonneau M, Subramanian S, Seedorf H, Goodman AL, Clemente JC, Knight R, Heath AC, Leibel RL, et al. The long-term stability of the human gut microbiota. Science (80-). 2013;341:1237439.
16. Zhang J, Ding X, Guan R, Zhu C, Xu C, Zhu B, Zhang H, Xiong Z, Xue Y, Tu J, et al.

Evaluation of different 16S rRNA gene V regions for exploring bacterial diversity in a eutrophic freshwater lake. Sci Total Environ. 2018;618:1254–67.
17. Caporaso JG, Lauber CL, Walters WA, Berg-Lyons D, Lozupone CA, Turnbaugh PJ, Fierer N, Knight R. Global patterns of 16S rRNA diversity at a depth of millions of sequences per sample. Proc Natl Acad Sci. 2011;108.
18. Caporaso JG, Kuczynski J, Stombaugh J, Bittinger K, Bushman FD, Costello EK, Fierer N, Peña AG, Goodrich JK, Gordon JI, et al. QIIME allows analysis of high-throughput community sequencing data. Nat Methods. 2010;7:335–6.
19. Subramanian A, Tamayo P, Mootha VK, Mukherjee S, Ebert BL, Gillette MA, Paulovich A, Pomeroy SL, Golub TR, Lander ES, et al. Gene set enrichment analysis: A knowledge-based approach for interpreting genome-wide expression profiles. Proc Natl Acad Sci. 2005;102:15545–50.
20. Olson C a., Vuong HE, Yano JM, Liang QY, Nusbaum DJ, Hsiao EY. The gut microbiota mediates the anti-seizure effects of the ketogenic diet. Cell. 2018;173:1728–41.
21. Gregory JC, Buffa JA, Org E, Wang Z, Levison BS, Zhu W, Wagner MA, Bennett BJ, Li L, DiDonato JA. Transmission of atherosclerosis susceptibility with gut microbial transplantation. J Biol Chem. 2015;290:5647–60.
22. Suez J, Korem T, Zeevi D, Zilberman-Schapira G, Thaiss CA, Maza O, Israeli D, Zmora N, Gilad S, Weinberger A, et al. Artificial sweeteners induce glucose intolerance by altering the gut microbiota. Nature. 2014;514:181–6.
23. Lozupone C, Knight R. UniFrac: a new phylogenetic method for comparing microbial communities. Appl Environ Microbiol. 2005;71:8228–35.
24. Oksanen J, Blanchet FG, Kindt R, Legendre P, Minchin PR, O'Hara RB, Simpson GL, Solymos P, Stevens MH, Wagner H. vegan: community ecology package. 2014.
25. Parks DH, Tyson GW, Hugenholtz P, Beiko RG. STAMP : statistical analysis of taxonomic and functional profiles. 2014;30:3123–4.
26. Segata N, Izard J, Waldron L, Gevers D, Miropolsky L, Garrett WS, Huttenhower C. Metagenomic biomarker discovery and explanation. Genome Biol. 2011;12:R60.
27. White JR, Nagarajan N, Pop M. Statistical methods for detecting differentially abundant features in clinical metagenomic samples. PLoS Comput Biol. Public Library of Science; 2009;5:e1000352.
28. Storey JDD, Taylor JE, Siegmund D. Strong control, conservative point estimation and simultaneous conservative consistency of false discovery rates: a unified approach. J R Stat Soc. 2004;66:187–205.
29. Zheng CH, Yuan L, Sha W, Sun ZL. Gene differential coexpression analysis based on biweight correlation and maximum clique. BMC Bioinformatics. 2014;15:S3.
30. Reed DR, Li S, Li X, Huang L, Tordoff MG, Starling-Roney R, Taniguchi K, West DB, Ohmen JD, Beauchamp GK, et al. Polymorphisms in the taste receptor gene (Tas1r3) region are associated with saccharin preference in 30 mouse strains. J Neurosci. 2004;24:938–46.
31. Kootte RS, Levin E, Salojärvi J, Smits LP, Hartstra A V, Udayappan SD, Hermes G, Bouter KE, Koopen AM, Holst JJ, et al. Improvement of insulin sensitivity after lean donor feces in metabolic syndrome is driven by baseline intestinal microbiota composition. Cell Metab. 2017;26:611–9.
32. Dao MC, Everard A, Aron-Wisnewsky J, Sokolovska N, Prifti E, Verger EO, Kayser BD, Levenez F, Chilloux J, Hoyles L, et al. Akkermansia muciniphila and improved metabolic

health during a dietary intervention in obesity: relationship with gut microbiome richness and ecology. Gut. 2016;65:426–36.
33. Ley RE, Backhed F, Turnbaugh P, Lozupone CA, Knight RD, Gordon JI. Obesity alters gut microbial ecology. Proc Natl Acad Sci U S A. 2005;102:11070–5.
34. Wahlström A, Sayin SI, Marschall H-U, Bäckhed F. Intestinal crosstalk between bile acids and microbiota and its impact on host metabolism. Cell Metab. 2016;24:41–50.
35. Derrien M, van Baarlen P, Hooiveld G, Norin E, Muller M, de Vos W. Modulation of Mucosal Immune Response, Tolerance, and Proliferation in Mice Colonized by the Mucin-Degrader Akkermansia muciniphila. Front Microbiol. 2011;2:166.
36. Everard A, Belzer C, Geurts L, Ouwerkerk JP, Druart C, Bindels LB, Guiot Y. Cross-talk between *Akkermansia muciniphila* and intestinal epithelium controls diet-induced obesity. Proc Nati Acad Sci USA. 2013;110:9066–71.
37. Org E, Parks BW, Joo JWJ, Emert B, Schwartzman W, Kang EY, Mehrabian M, Pan C, Knight R, Gunsalus R. Genetic and environmental control of host-gut microbiota interactions. Genome Res. 2015;25:1558–69.
38. Jost T, Lacroix C, Braegger CP, Chassard C. New insights in gut microbiota establishment in healthy breast fed neonates. PLoS One. 2012;7.
39. Krych, Nielsen DS, Hansen AK, Hansen CHF. Gut microbial markers are associated with diabetes onset, regulatory imbalance, and IFN-γ level in NOD Mice. Gut Microbes. 2015;6:101–9.
40. Payne AN, Chassard C, Lacroix C. Gut microbial adaptation to dietary consumption of fructose, artificial sweeteners and sugar alcohols: implications for host–microbe interactions contributing to obesity. Obes Rev. 2012;13:799–809.
41. Levine UY, Looft T, Allen HK, Stanton TB. Butyrate-producing bacteria, including mucin degraders, from the swine intestinal tract. Appl Environ Microbiol. 2013;79:3879–81.
42. Peng L, Li Z-R, Green RS, Holzman IR, Lin J. Butyrate enhances the intestinal barrier by facilitating tight junction assembly via activation of AMP-activated protein kinase in Caco-2 cell monolayers. J Nutr. 2009;139:1619–25.
43. Moreno-Indias I, Sánchez-Alcoholado L, García-Fuentes E, Cardona F, Queipo-Ortuño MI, Tinahones FJ. Insulin resistance is associated with specific gut microbiota in appendix samples from morbidly obese patients. Am J Transl Res. 2016;8:5672–84.
44. Lamar E, Deblandre G, Wettstein D, Gawantka V, Pollet N, Niehrs C, Kintner C. Nrarp is a novel intracellular component of the Notch signaling pathway. Genes Dev. 2001;15:1885–99.
45. Olszewski PK, Klockars A, Schiöth HB, Levine AS. Oxytocin as feeding inhibitor: Maintaining homeostasis in consummatory behavior. Pharmacol Biochem Behav. 2010;97:47–54.
46. Zhang X, Van Den Pol AN. Hypothalamic arcuate nucleus tyrosine hydroxylase neurons play orexigenic role in energy homeostasis. Nat Neurosci. 2016;19:1341–7.
47. Xia W, Pessentheiner AR, Hofer DC, Amor M, Schreiber R, Schoiswohl G, Eichmann TO, Walenta E, Itariu B, Prager G, et al. Loss of ABHD15 impairs the anti-lipolytic action of insulin by altering PDE3B stability and contributes to insulin resistance. Cell Rep. 2018;23:1948–61.
48. Shimizu I, Yoshida Y, Moriya J, Nojima A, Uemura A, Kobayashi Y, Minamino T. Semaphorin3E-induced inflammation contributes to insulin resistance in dietary obesity. Cell Metab. 2013;18:491–504.

49. Cavallari, J. F., Anhe, F. F., Foley , K. P., Denou E., Chan R. W., Bowdish D. M. E. SJD. Targeting macrophage scavenger receptor 1 promotes insulin resistance in obese male mice. 2018;6:1–11.
50. Qi L, Saberi M, Zmuda E, Wang Y, Altarejos J, Dentin R, Hedrick S, Bandyopadhyay G, Hai T, Montminy M. Adipocyte CREB promote insulin resistance in obesity. Cell Metab. 2010;9:277–86.
51. Wueest S, Rapold R a., Schumann DM, Rytka JM, Schildknecht A, Nov O, Chervonsky A V., Rudich A, Schoenle EJ, Donath MY, et al. Deletion of Fas in adipocytes relieves adipose tissue inflammation and hepatic manifestations of obesity in mice. J Clin Invest. 2010;120:191–202.

Table 1. Differentially abundant microbiota between fructose and water groups in cecal and fecal samples of B6, DBA, and FVB mice.

Mouse strain	Taxonomic level	Source	Fructose-responsive microbiota	Fold change
DBA	Family	Cecum	Erysipelotrichaceae	0.055*
B6	Family	Feces	Rikenellaceae	0.620*
	Family	Feces	S24-7	1.19*
	Family	Feces	Dehalobacteriaceae	0.600*
	Family	Feces	Lachnospiraceae	0.590*
	Family	Feces	Mogibacteriaceae	0.333*
	Family	Feces	Ruminococcaceae	0.706*
	Family	Feces	Turicibacteraceae	0.348*
	Family	Feces	Pseudomonadaceae	3.33*
	Family	Feces	Verrucomicrobiaceae	7.25**
DBA	Family	Feces	Rikenellaceae	0.374*
	Family	Feces	Pseudomonadaceae	33.3*
DBA	Genus	Cecum	*Erysipelotrichaceae (Unknown genus)*	0.004*
	Genus	Cecum	*Erysipelotrichaceae Clostridium*	0.009**
	Genus	Cecum	*Lachnospiraceae Anaerostipes*	0.025**
FVB	Genus	Cecum	*Bifidobacteriaceae Bifidobacterium*	16.5*
B6	Genus	Feces	*Dehalobacteriaceae Dehalobacterium*	0.600*
	Genus	Feces	*Mogibacteriaceae (Unknown genus)*	0.333*
	Genus	Feces	*Verrucomicrobiaceae Akkermansia*	7.27**
DBA	Genus	Feces	*Rikenellaceae (Unknown genus)*	0.374*
	Genus	Feces	*Pseudomonadaceae (Unknown genus)*	60.0*
	Genus	Feces	*Pseudomonadaceae Pseudomonas*	28.0*

[1]Fold change is calculated as the ratio of the relative abundance of microbiota between fructose and water groups (fructose/water). *n*=8/group/mouse strain, *FDR < 0.05, **FDR < 0.01.

Table 2. Correlation between fructose-responsive microbiota and host fructose signature genes in three metabolic tissues in B6 and DBA mice.

Mouse strain	Fructose-responsive microbiota	Host tissue	No. correlated Gene at FDR <0.05	Correlation with host fructose-responsive genes	
				Top correlated genes	Over-represented pathways
B6 (feces)	Rikenellaceae	Hypo	37	*Emg1, Rpl37a, Oat, Gna13,* ***Ctsz***	RNA metabolism, Protein localization in endoplasmic reticulum, Ribosome, Amino acid metabolism, Influenza infection
	S24-7	Hypo	11	***Numbl, Cxx1c, Gnb2, 1500009L16Rik, Slc25a17***	
	Dehalobacteriaceae	Hypo	7	***Atp2b2, Slc6a3, Nefh,*** *Nrarp, Hint2*	
	Dehalobacterium	Hypo	42	***Atp2b2, Slc6a3, Nefh,*** *Nrarp,* ***Atg3,***	Ribosome, Response to alcohol, Blood circulation, Dopamine biosynthesis, Locomotory behavior
	Lachnospiraceae	Hypo	2	*Maneal, Rbm39*	
	Mogibacteriaceae	Hypo	54	*Mogs, Snrpe, Nrarp,* ***Timp3****, Sgsm1*	Ribosome, Metabolism of proteins, RNA, organonitrogen compound, Protein targeting to membrane metabolism
	Mogibacteriaceae (Unknown genus)	Hypo	130	*Mogs, Psmb4, Derl1,* ***Timp3****, Sdcbp*	Ribosome, Metabolism of protein, RNA, Protein localization to endoplasmic reticulum, Signaling by robo receptors
	Ruminococcaceae	Hypo	12	*Trappc2l, Gnb2, Uck1, Mid1ip1,* ***Itm2a***	
	Pseudomonadaceae	Hypo	2	***Cxx1c, Numbl***	
	Verrucomicrobiaceae	Hypo	13	***Scarna2, AW209491,*** *Gja1,* ***Rps9,*** *Th,*	Ribosome, Protein localization to endoplasmic reticulum, mRNA activation
	Akkermansia	Hypo	44	*Gja1,* ***Rps9,*** *Th, Bmp7,* ***Oxt***	Ribosome, Protein localization to endoplasmic reticulum, Selenoamino acid metabolism, Influenza infection, Signaling by robo receptors
DBA (cecum)	*Erysipelotrichaceae (Unknown genus)*	Liver	5	***Gsdmd, Wdr82, Tmem62, S100a10, Pgk1,***	
	Erysipelotrichaceae Clostridum	Liver	5	***Epha2, Mad2l2, Cyp8b1, Ero1l, Pus10***	
	Lachnospiraceae Anaerostipes	Liver	4	***Rogdi, Cyp8b1, Mad2l2, Baiap2***	
DBA (feces)	Rikenellaceae	Adipose	447	*Ccr1, Sema3e, Msr 1, Abhd3, Fas,*	RNA metabolism, Response to lipid, cytokines, bacterial molecule, Lipid metabolism, Immune system, Endocytosis

Rikenellaceae (Unknown genus)	Adipose	432	*Ccr1, Apobec1, Sema3e, Creb1, Fas*	RNA metabolism, Response to lipid, cytokines, bacterial molecule, Lipid metabolism, Immune system, Signaling pathway
Pseudomonadaceae	Adipose	77	***Sfrp4, Msr1, Sema3e, Abhd3, Fas***	
Pseudomonadaceae (Unknown genus)	Adipose	209	***Creb1, Fabp3, Msr1, Sema3e, Fas***	RNA processing, Response to cytokine, lipid, Defense response, lipid metabolism, Response to hormone
Pseudomonas	Adipose	43	***Ppp1r13b, Jmjd1c, Msr1, Slc25a10, Fabp3***	

[1]Fructose-responsive genes in Hypothalamus (Hypo), Liver, and Adipose which were positively or negatively correlated with microbiota were indicated in bold or non-bold font, respectively.
[2]Top five correlated genes which belong to major gene sets analyzed using GSEA software.
[3]Sample size *n*=4-6/group/mouse strain.
[4]Full lists of correlated genes are in Supplemental Table 1 and enriched pathways are in Supplemental Table 2.

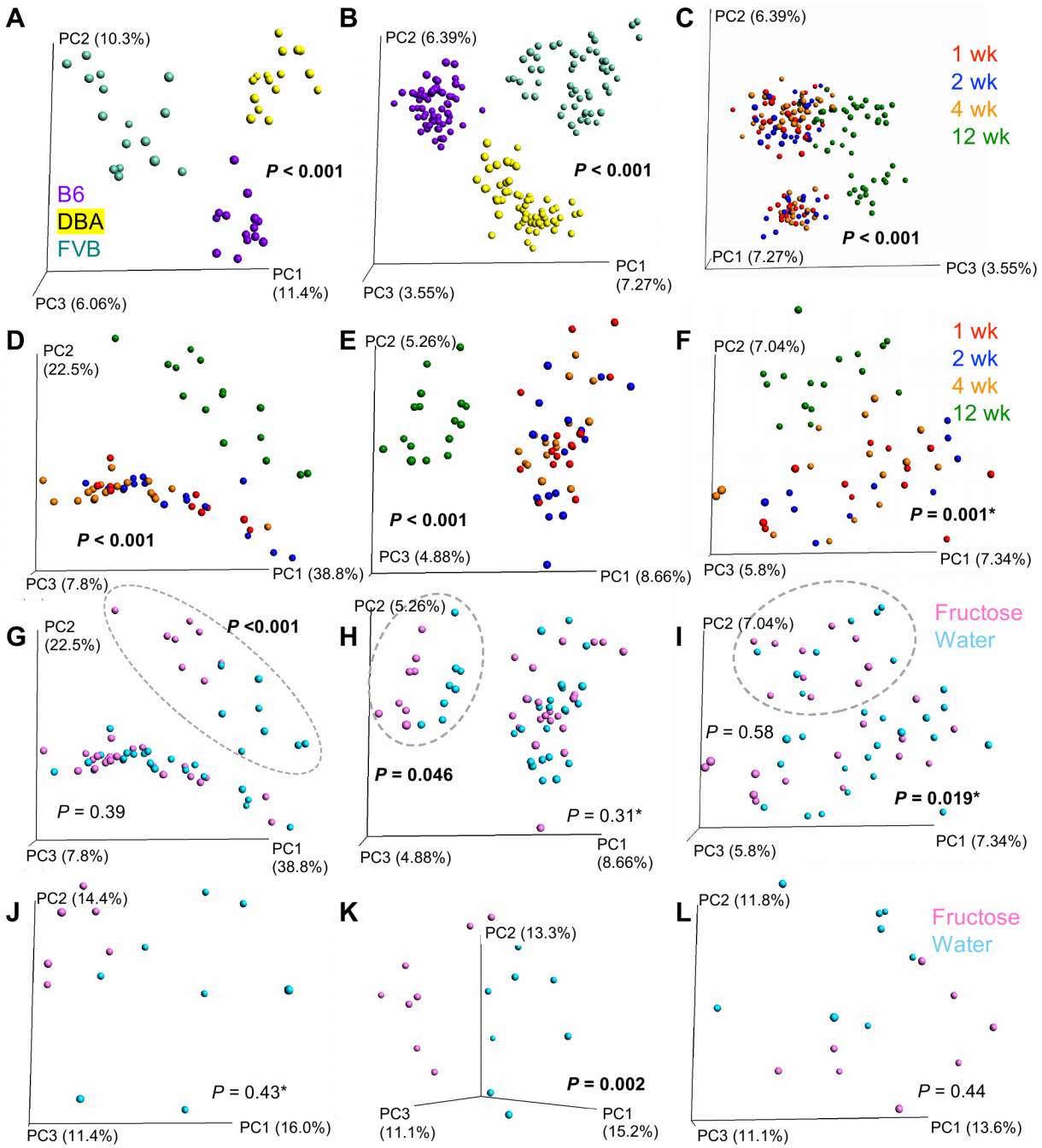

Figure 1. Principal coordinates analysis (PCoA) of cecal and fecal microbiota of B6, DBA, and FVB mice consuming fructose or regular water. (A) Cecal microbiota samples across three mouse strains were shown to separate by strain (A; *n* = 16/strain; week 12). (B-C) Fecal microbiota samples across three mouse strains were separated by both strain (B; *n* = 64/strain

across 4 time points) and time (C; n = 16/time point for each strain). Plot C used the same ordination as plot B, except principal coordinate 3 (PC3) was presented as the x-axis to show the relationship with time. (D-F) For each mouse strain, fecal samples were colored by time points for B6 (D), DBA (E), and FVB (F) to show the time effect. (G-I) Fecal samples were colored with fructose or water treatment for B6 (G), DBA (H), and FVB (I) to show treatment effect. Samples for the 12-week time point were shown in dotted circles, with the corresponding *P*-values for fructose treatment effect reported. (J-L) Cecal samples were colored by the fructose or water treatment for B6 (J), DBA (K), and FVB (L). *P*-values were generated by PERMANOVA, and significant results were presented in bold. *P*-values with an asterisk designate that significantly different dispersions were observed, which may influence the *P*-values reported as PERMANOVA assumes similar dispersion.

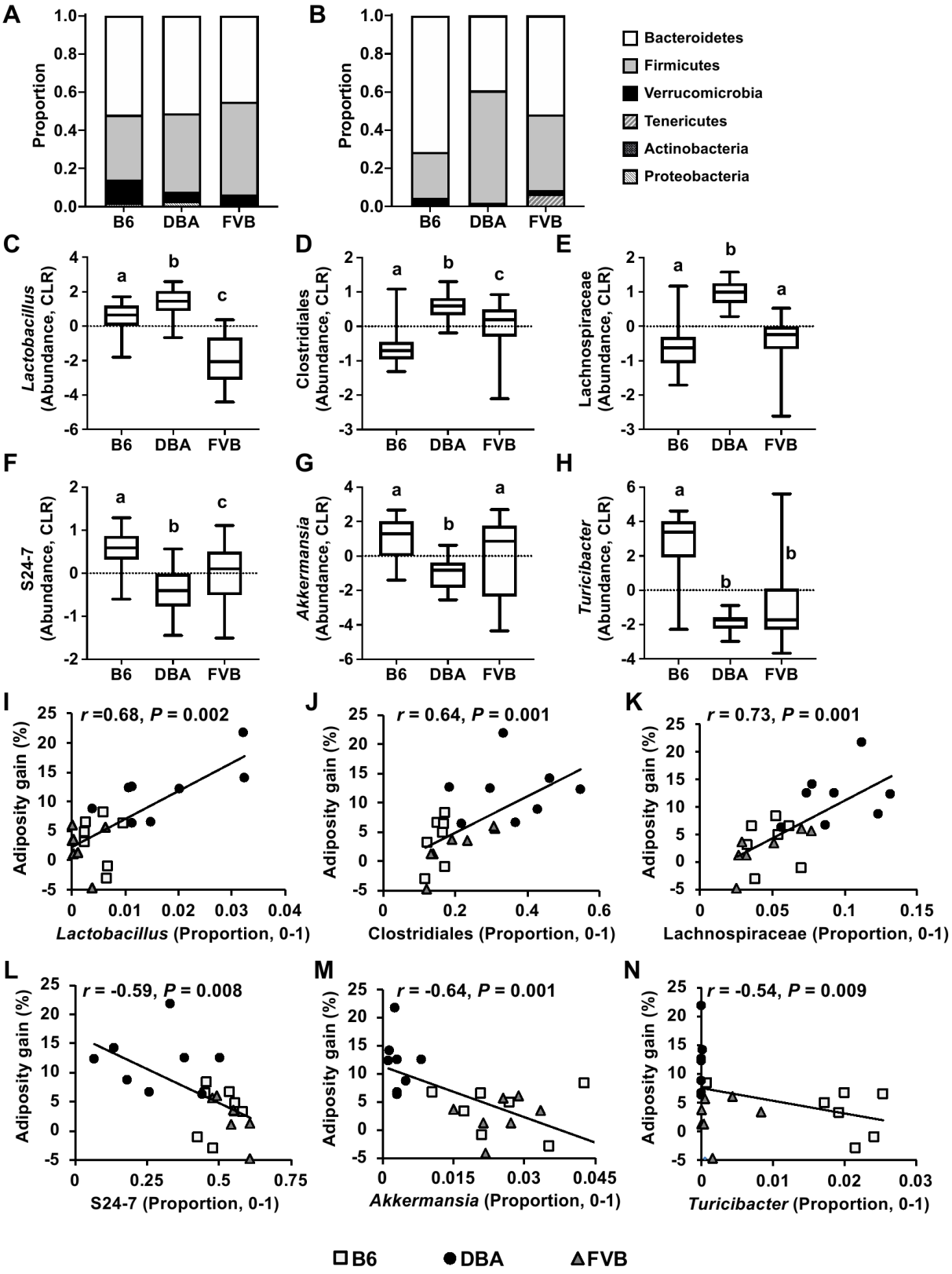

Figure 2. Cecal and fecal baseline microbial composition in B6, DBA, and FVB mice and

correlation with adiposity gain. (A-B) Taxa bar plots of baseline cecal (A) and fecal (B) microbiota of three mouse strains at the phylum level. (C-H) Baseline abundance profiles for specific fecal microbiota of three mouse strains at the genus level. Centered log-ratio (CLR) values were used for plotting the abundance of each microbiota. Box and whiskers plots from minimum to maximum showing abundance distribution of *Lactobacillus* (C), unknown genus of Clostridiales (D), unknown genus of Lachnospiraceae (E), unknown genus of S24-7 (F), *Akkermansia (*G), and *Turicibacter* (H). The center line in the box denotes the median value. One-way ANOVA followed by Sidak's post hoc test was conducted to calculate significant differences between three mouse strains. Labeled means without a common letter differ, $P < 0.05$. n = 7-8/group. (I-N) Correlation analysis plots between microbiota baseline proportion and adiposity gain at week 12 of fructose treatment. r = Biweight midcorrelation (*bicor*) coefficient, P = Benjamini-Hochberg adjusted P-values. n = 7-8/mouse strain.

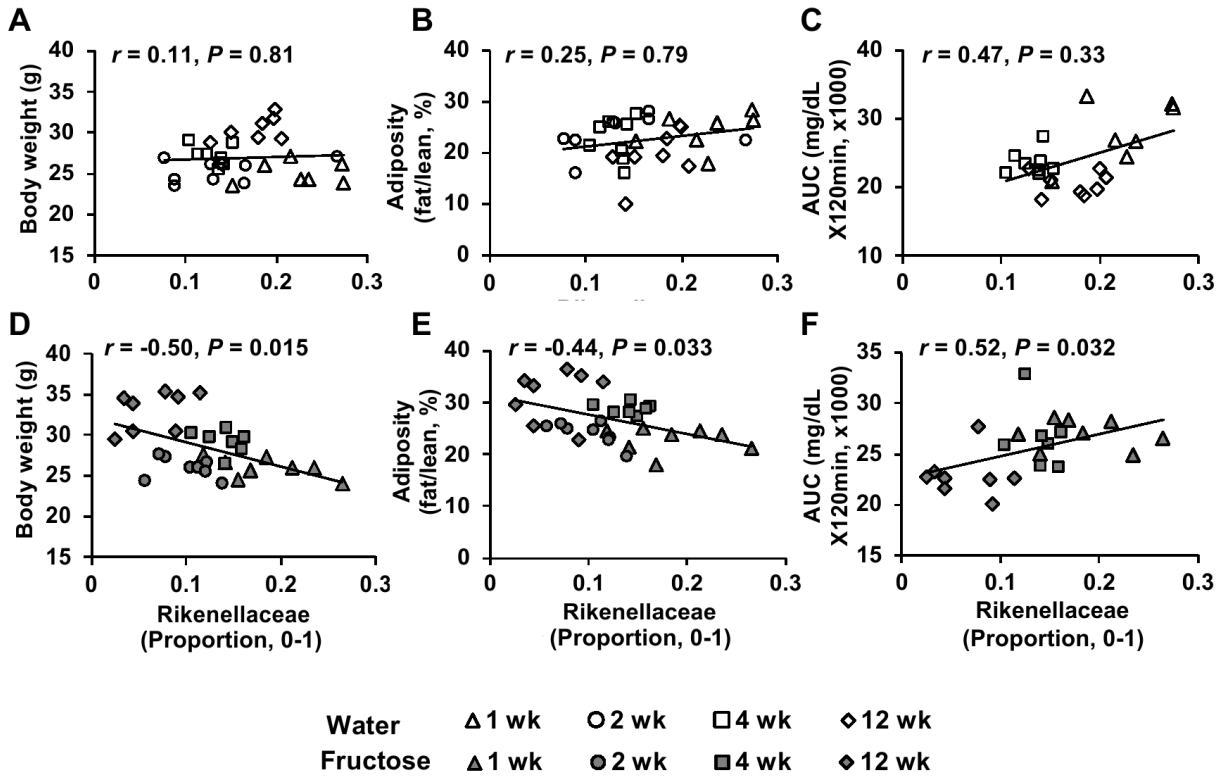

Figure 3. Correlation analysis of fructose-responsive microbiota with metabolic phenotypes in DBA mice. (A-C) Correlation plots between Rikenellaceae proportion and body weight (A), adiposity (B), and glucose tolerance AUC (C) across time points in the water group. (D-F) Correlation plots between Rikenellaceae proportion and body weight (D), adiposity (E), and glucose tolerance AUC (F) across time points in the fructose group. *r* = Biweight midcorrelation (*bicor*) coefficient, *P* = Benjamini-Hochberg adjusted *P*-values. *n* = 7-8/group/time point.

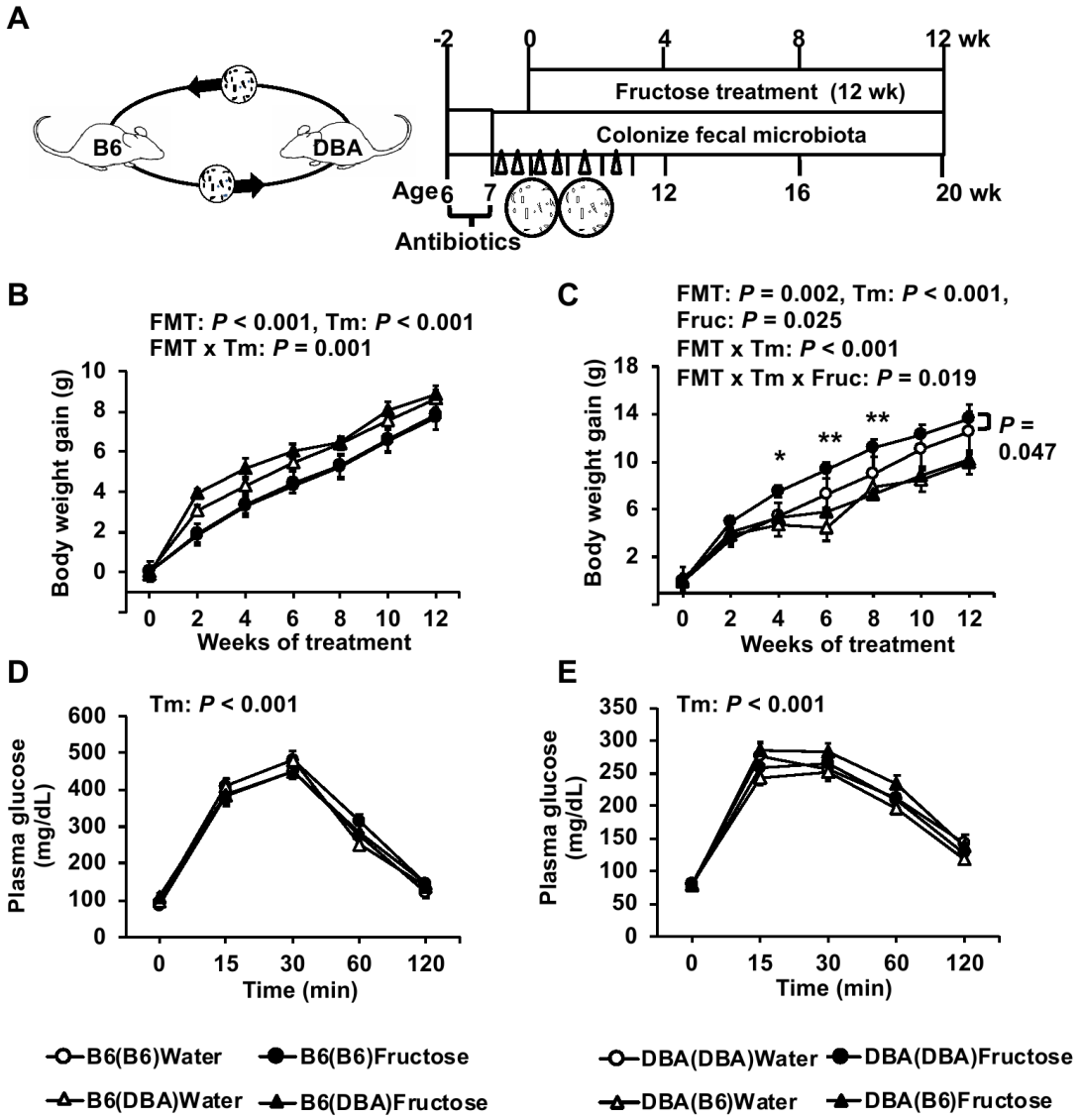

Figure 4. Metabolic phenotypes post fecal transplant in B6 and DBA mice with or without fructose consumption. (A) Schematic design of fecal microbiota transplant (FMT). (B-E) Body weight gain (B, C) and glucose tolerance (D, E) of recipient B6 and DBA mice, respectively, with or without 8% fructose water. Data are presented as means ± SEM, *n* = 7-14/group. The *P*-values of the main factors (FMT, fructose, time) and interactions by three-way repeated-measures ANOVA are shown on the top of the graph. Asterisks in (C) indicate time points at which significant differences were found between DBA(DBA) and DBA(B6) under fructose

treatment based on two-way repeated-measures ANOVA with Sidak's post hoc test; *$P < 0.05$, **$P < 0.01$. Fructose effects within each FMT group across time points were assessed by two-way repeated-measures ANOVA, and significant difference between fructose and water treatments for the DBA(DBA) FMT group is indicated by a *P*-value with a side bar (C). B6(B6): B6 mice receiving B6 feces; B6(DBA): B6 mice receiving DBA feces; DBA(B6): DBA mice receiving B6 feces; DBA(DBA): DBA mice receiving DBA feces; Fruc: Fructose; Tm: Time.

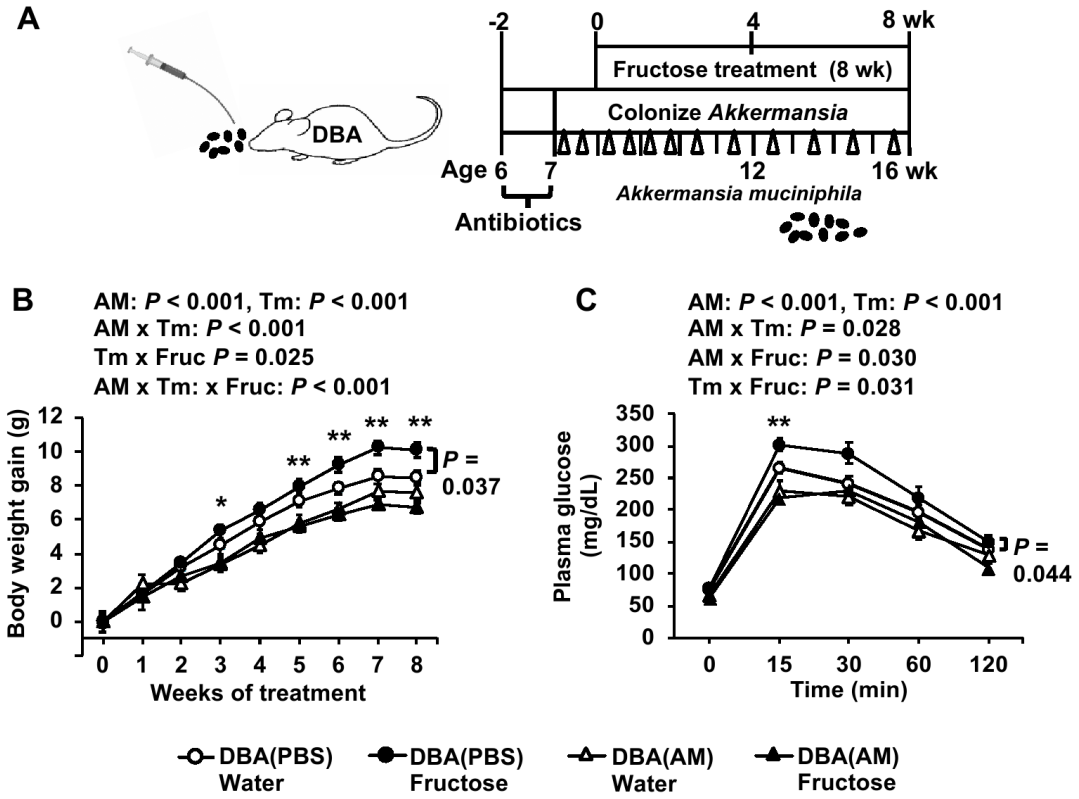

Figure 5. Metabolic phenotypes post *Akkermansia* colonization in DBA mice with or without fructose consumption. (A) Schematic design of *Akkermansia muciniphila* (AM) colonization. PBS serves as the control for AM. (B-C) Body weight gain (B) and glucose tolerance (C) of recipient DBA mice with or without 8% fructose water. Data are presented as means ± SEM, n = 8-14/group. The P-values of main factors (AM, fructose, time) and interactions by three-way repeated-measures ANOVA are shown on the top of the graph. Asterisks indicate time points at which significant differences were found between the AM colonization and PBS control groups under fructose treatment based on two-way repeated-measures ANOVA with Sidak's post hoc test; *$P < 0.05$, **$P < 0.01$. Fructose effects within PBS or AM group across time points were assessed by two-way repeated-measures ANOVA. A significant fructose effect on weight gain and glucose tolerance in mice receiving PBS is indicated by a P-values with a side bar (B and C). Fruc: Fructose; Tm: Time.